

Supplementary Information

**A scalable on-demand platform to assemble base nanocarriers for
combination cancer therapy**

*Milan Gautam,^a Sae Kwang Ku,^b Jong Oh Kim^{*a} and Jeong Hoon Byeon^{*c}*

^aCollege of Pharmacy, Yeungnam University, Gyeongsan 38541, Republic of Korea

^bCollege of Korean Medicine, Daegu Haany University, Gyeongsan 38610, Republic of Korea

^cSchool of Mechanical Engineering, Yeungnam University, Gyeongsan 38541, Republic of Korea

*Corresponding authors: postjb@yu.ac.kr and jongohkim@yu.ac.kr

Preparation of GO-yTiO₂@DP NCs

To prepare yTiO₂ NVs first, hydrogen flame [1.5 L min⁻¹ hydrogen, 0.5 L min⁻¹ air for TiCl₄ vaporization, and 8.0 L min⁻¹ air were co-injected into a quartz burner (141/18/60, Arnold Gruppe, Germany)]-synthesized TiO₂ NPs were directly supplied into a reactor with flowing H₂O₂ solution (1 min residence time). An ultrasound probe (VCX 750, 20 kHz, Sonics and Materials Inc., USA) was installed inside the reactor, and the direction of the ultrasound countered the TiO₂ NP-laden flow to immediately collapse the bubbles generated by the flow, resulting in the hydrosolization of TiO₂ NPs. The dispersed TiO₂ NPs were then reacted with H₂O₂ for 1 min to form yTiO₂ NVs. The reacted solution was mechanically sprayed out with pure nitrogen gas flow and entered an activated carbon-silica gel-packed hollow tube to remove residual H₂O₂. The yTiO₂-laden nitrogen flow was used to operate another mechanical spray device containing a mixture solution of GO, D, and P for the generation of hybrid droplets. The droplets were then passed through a heated tubular reactor to extract solvent from the droplets to form GO-yTiO₂@DP NCs (**Fig. S1**). The NCs in the gas flow were positively charged via field charging (pin-to-cylinder corona charging), and the charged NCs were finally precipitated on a polished duralumin rod (negative potential) as powder form via electrostatic attraction. The sampling rod was immersed in buffered saline under bath sonication to form NC dispersion before bioassays.

Characterization

Physicochemical property

The aerosol size distributions of yTiO₂, GO@DP, and GO-yTiO₂@DP samples were analyzed using SMPS (3936, TSI, USA). Morphologies of the samples were observed by TEM (Tecnai G2 F20 S-TWIN, FEI, USA) upon the samples were directly deposited on carbon-coated copper grids (Tedpella, USA) in the aerosol state. The light absorption spectra of the samples dispersed in PBS were measure by UV-Vis spectrophotometer (T60, PG Instruments, UK). The crystallinity of TiO₂ and yTiO₂ was confirmed using XRD (D/MAX-2500, Rigaku, Japan) and Raman spectroscopy (XploRA Plus, Horiba, Japan). The surface structures of TiO₂, yTiO₂, and GO were examined using XPS (Axis-HIS, Kratos Analytical, Japan).

EE and LC

The entrapment of D in GO@DP and GO-yTiO₂@DP samples was determined by separating the free D from the D loaded samples using an Amicon centrifugal ultrafiltration device (MWCO 10000 D_a, Millipore, USA) at 5000 rpm for 10 min. The concentration of the D was measured at a wavelength of 485 nm using UV-Vis spectrophotometer (U-2800, PerkinElmer, Japan). The % EE and LC of the D were determined using following formula:

$$EE (\%) = W_{ED} / W_{TD} \times 100$$

$$LC (\%) = W_{TD} - W_{UD} / W_{TS} \times 100$$

where, W_{ED} , W_{TD} , W_{UD} , and W_{TS} are the weights of the D entrapped in the samples, total D, unbound D, and total samples, respectively.

Photothermal activity

The photothermal activities of GO@DP and GO-yTiO₂@DP samples were measured by using a fiber-coupled infrared laser power supply (Changchun New Industries Optoelectronics Technology, China). The thermal images and temperature contour of each sample were obtained by thermal camera (Therm-App TH, Opgal Optronic Industries, Ltd., Isreal) fixed at a distance of 10 cm from the laser module. The samples were dispersed in the DMEM media (100 µg mL⁻¹), constant laser power (2.0 W cm⁻² power density) was irradiated on the samples, and the temperature profiles were recorded.

D release

In vitro release profiles of D from GO@DP and GO-yTiO₂@DP samples were evaluated in PBS (pH 7.4) and ABS (pH 5.0) via diffusion method. Briefly, 1 mL of GO@DP or GO-yTiO₂@DP dispersion (equivalent to 0.5 mg) was sealed in a dialysis bag (MWCO 3500 D_a) and placed in a 25 ml release media in a water bath shaker with a stirring rate of 100 rpm at 37°C. At predetermined time periods, aliquots of samples (0.5 mL) were withdrawn, followed by replenishment with an equal amount of fresh media. The percentage of released D from the samples was determined using UV-Vis spectroscopy.

Bioassay

Cytotoxicity

Cell viabilities of D, GO, yTiO₂, GO-yTiO₂, GO@DP, and GO-yTiO₂@DP samples were assessed in SCC-7 (squamous cell carcinoma) cell line via MTT assay in absence and presence of NIR irradiation. 10⁴ SCC-7 cells per well were seeded in 96-well plate and incubated overnight for cell attachment. After 48 h treatment, the cells were washed twice with PBS and treated with 100 µL MTT reagent (1.25 mg mL⁻¹ each well). After 4 h incubation, violet colored formazan crystals were dissolved with 100 µL cell grade dimethyl sulfoxide, and the absorbance was measured at 570 nm using a microplate reader (Multiskan EX, Thermo Scientific, USA). The percentage cell viability was calculated as $A_{\text{sample}}/A_{\text{control}} \times 100$, where A represents the absorbance at 570 nm.

Intracellular trafficking

The qualitative cellular uptake of samples in SCC-7 cells was studied using CLSM (K1-Fluo, Nanoscope System, Inc., Korea). SCC-7 cells (2 × 10⁴ cells per well) were seeded on coverslips placed in the 12-well and incubated for 24 h, followed by the addition of GO@DP and GO-yTiO₂@DP (equivalent to 5 µg mL⁻¹ D) samples to each well. After incubation at different time intervals (5, 10, and 15 min), the cells were treated with 100 ng lysotracker green, washed with PBS, and fixed on 4% paraformaldehyde solution in dark. The coverslips were then washed with PBS, mounted on glass slides and sealed with glycerin. To perform the qualitative intracellular uptake, SCC-7 cells were (1 × 10⁵ cells per well) seeded onto 12-well plates and incubated for 24 h. The cells were treated with GO@DP and GO-yTiO₂@DP samples at different time- and concentration-dependent manner at 37°C. After incubation, the cells were then washed with PBS, harvested by trypsinization, and resuspended in 1 mL of PBS for flow cytometry analysis using FACS flow cytometer (BD Bioscience, USA).

Live/dead assay

To analyze the apoptosis, SCC-7 cells were separately inoculated in 12-well plates and incubated for 24 h to allow cell attachment. The treatment of cells was then performed with D, GO@DP, and GO-

yTiO₂@DP samples in the absence and presence of NIR irradiation. After 24 h, the cells were stained with acridine orange and propidium iodide solutions at 6.7 and 750 μM concentrations, respectively. The cells were washed with PBS and observed under the fluorescence microscope (Eclipse Ti, Nikon Instruments, Inc., USA).

Biodistribution and photothermal imaging

In order to assess the *in vivo* biodistribution of Cy5.5 loaded GO@DP and GO-yTiO₂@DP samples, SCC-7 xenograft tumor bearing mice were administered intravenously with appropriate dose. After intravenous administration, the distributions of samples were tracked at 1, 3, 6, 12, and 24 h using *in vivo* imaging system (FOBI, NeoScience Co., Ltd, Korea). The mice were scarified after 24 h, and the fluorescence intensity of the tumor tissue and major organs (heart, spleen, kidney, lung, and liver) of each mouse were analyzed to determine the localization of GO@DP and GO-yTiO₂@DP samples in the respective tissue. To check the *in vivo* photothermal effect, dispersion of the samples were injected via i.v route and photothermal images were taken with digital thermal camera (Therm-App TH, Isreal). An NIR laser of 808 nm wavelength (2.0 W cm⁻² power density) was applied on the surface of tumor after 24 h i.v injection for 5 min, and digital photographs were recorded to observe the *in vivo* photothermal activities.

Antitumor study

In vivo antitumor effect of D, GO@DP, and GO-yTiO₂@DP samples were evaluated in SCC-7 xenograft tumor bearing Balb/c nude mice. SCC-7 xenograft tumors were developed in 6-week old mice by subcutaneous injection of 1 × 10⁷ SCC-7 cells into the right flanks of the thighs. When the tumor grown to an approximate volume of 100 mm³, the mice were divided into one control (G1) and five experimental groups [G2: D, G3: GO@DP (NIR irradiated), G4: GO@DP, G5: GO-yTiO₂@DP (NIR irradiated) and G6: GO-yTiO₂@DP; six mice for each group]. The samples were injected in a dose equivalent to 5 mg D per kg body weight, whereas, control group was treated with normal saline. The mice were exposed to NIR (2 W cm⁻²) for 5 min on the surface of tumor after 24 h injection. Each treatment was performed through tail vein injection three times at an interval of three days. The tumor diameters in each group were measured with digital Vernier caliper, and the tumor volume was calculated using the formula: Volume = (length × width²) / 2. For systemic toxicological assessment, changes in body weight of mice were recorded at specified time intervals. All animal procedures were performed in accordance with the Guidelines for Care and Use of Laboratory Animals of Yeungnam University and approved by the Animal Ethics Committee of Yeungnam University.

Histopathological characterization

The xenografted SCC-7 tumor mass and organs were crossly trimmed (3–4 μm), embedded in paraffin, and stained with H&E for observations using optical microscopy (Eclipse 80i, Nikon, Japan).

Immunohistochemistry

The immunoreactivity changes in tumor masses against the apoptotic markers, cleaved caspase-3 and cleaved PARP, angiogenesis marker, CD31, and tumor cell proliferation marker, Ki-67 were analyzed using purified primary antibodies with avidin-biotin-peroxidase complex (ABC) and peroxidase substrate kit. Endogenous peroxidase activity was blocked by incubated in methanol and 0.3% H₂O₂ for

30 min, and non-specific binding of immunoglobulin was blocked with normal horse serum blocking solution (1 h) in humidity chamber after heating (95–100°C) based epitope retrievals in 10 mM citrate buffers (pH 6.0). Primary antisera were treated overnight (4°C), and then incubated with biotinylated secondary antibody and ABC reagents at room temperature (1 h). Finally, peroxidase substrate kit was used to react with sections for 3 min and washed thrice with 0.01 M PBS between each step. The percentage region occupied by cleaved caspase-3, cleaved PARP, CD31, and Ki-67 positive cells in the tumors were analyzed by automated image analyzer as % min⁻² of tumor mass.

Hemolytic toxicity

The hemolytic percentage of free D and D loaded samples were evaluated using spectrophotometry (λ_{max} : 540 nm) by calculating the hemoglobin amount in the supernatant of the RBC suspension after centrifugation. Whole blood was collected from mice in heparinized tube and centrifuged for 10 min at 3500 rpm to separate the RBCs from the blood. The cells were re-suspended in the normal saline (10 mL), and 1 mL of suspended RBC, 9 mL of normal saline and 9 mL of distilled water were added, which was considered to be positive and negative control, respectively. 0.1 mL of free D and D loaded samples (equivalent to 5 $\mu\text{g mL}^{-1}$ D) added to 8.9 ml of saline and 1 mL of RBC suspension. The tubes were allowed to incubate for 30 min at 37°C and centrifuged at 3500 rpm for 10 min. The supernatant liquid was collected, and absorbance was measured at 540 nm using UV-vis spectrophotometer. The percentage hemolysis was determined using the following formula:

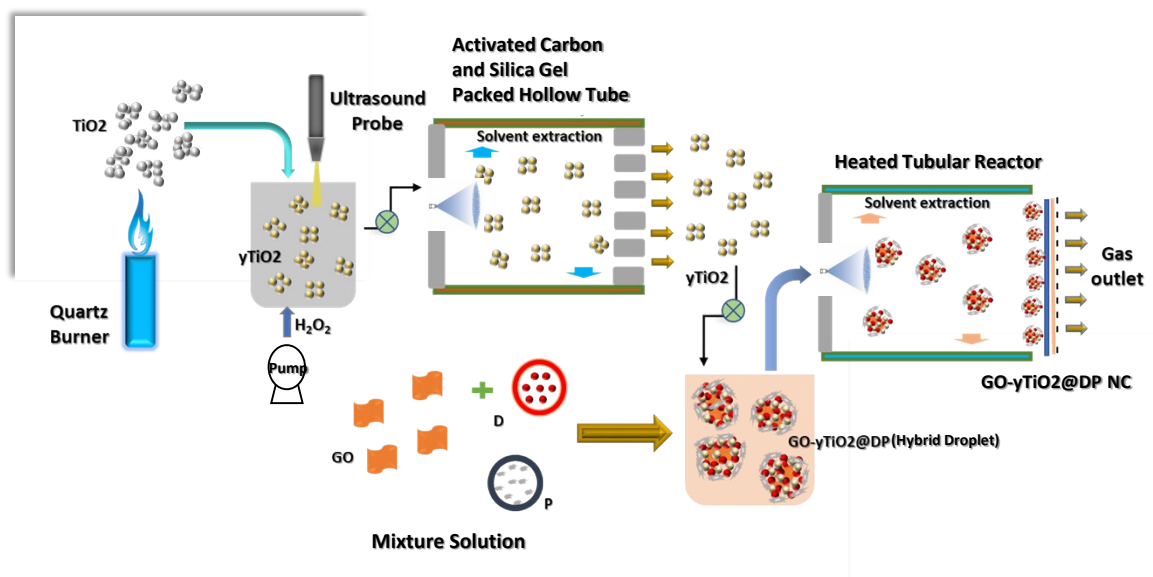
$$\% \text{ Hemolysis} = (\text{Abs} - \text{Abs}_0 / \text{Abs}_{100} - \text{Abs}_0) \times 100$$

where, Abs, Abs₀ and Abs₁₀₀ are the absorbances from each sample, negative control and positive control, respectively.

Dispersion stability

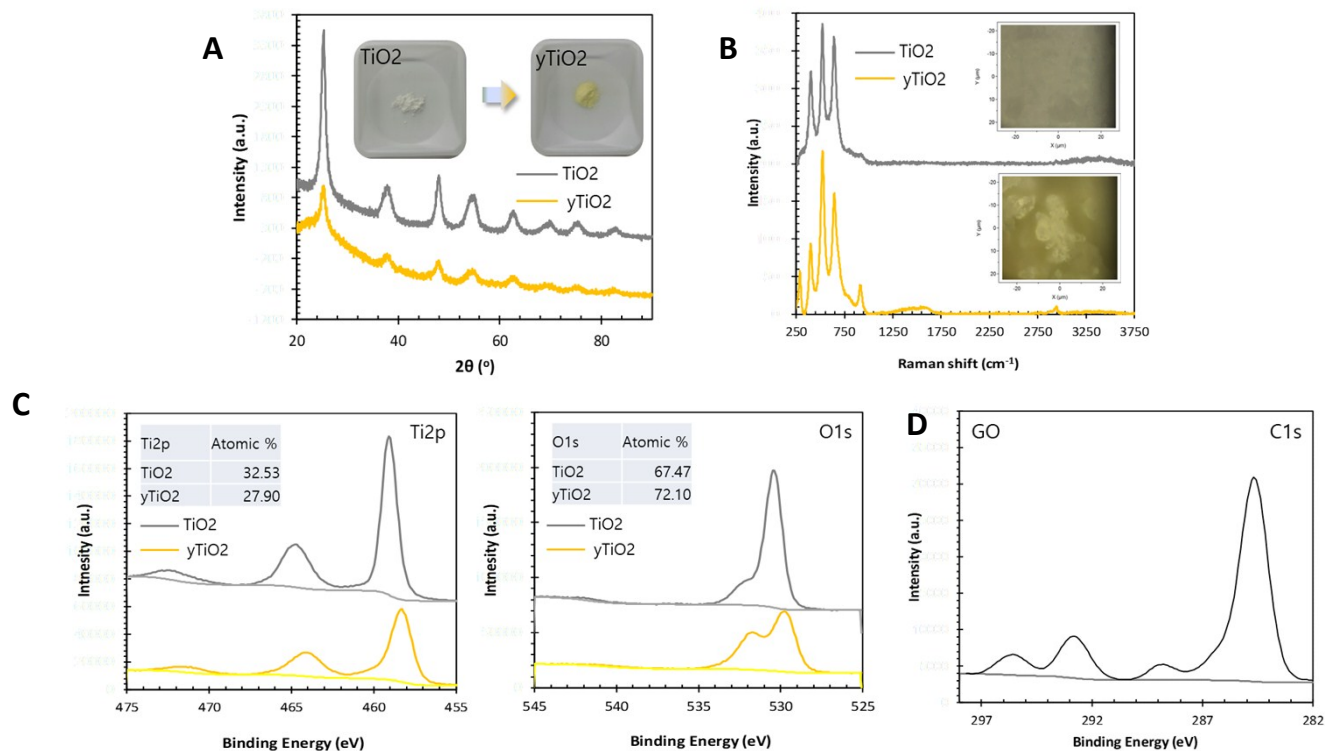
GO@DP and GO-yTiO₂@DP were dispersed into different dispersion media (PBS, DMEM, and FBS) to assess the stability of produced samples. The dispersions were placed under room temperature for 7 days and analyzed for any changes, such as color, turbidity, precipitation, and turbidity. Hydrodynamic particle size was measured using DLS (Nano ZS, Malvern Instruments, UK) system.

Fig. S1



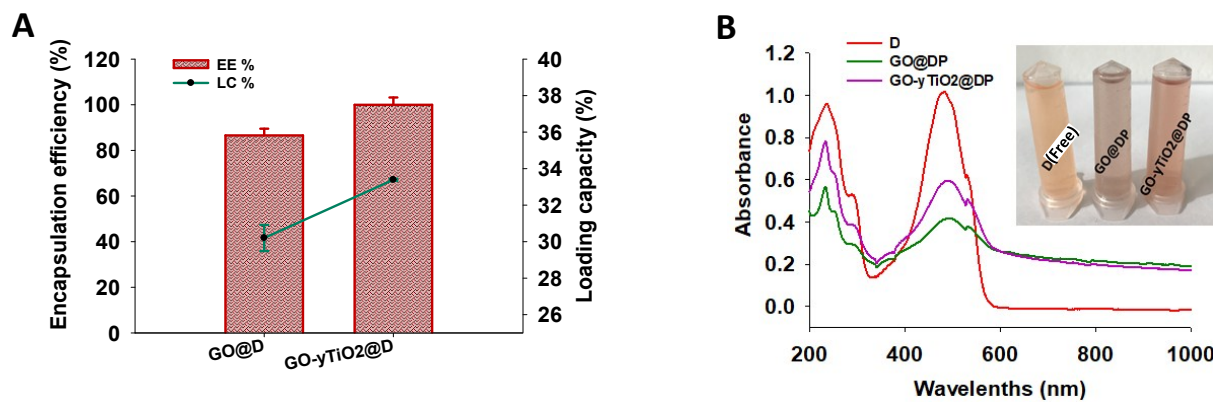
Aero-hydro-aero assembly of GO-yTiO₂@DP NCs. TiCl₄ was vaporized through air bubbling, and the vapor flow was then injected into a hydrogen diffusion flame. Ti⁴⁺ ions were converted to TiO₂ NPs near the flame, and the NP-laden flow was directly injected into H₂O₂ solution. The ultrasound collapsed bubbles generated by the NP-laden flow; therefore, the NPs were hydrosolized to be immediately reacted with H₂O₂ to form yTiO₂ NVs for 1 min. After passing through the hollow tube, the NV-laden flow was used as an operating fluid to produce droplets of GO-D-P mixture solution. During droplet generation, yTiO₂ NVs were incorporated in the droplets, and GO-yTiO₂@DP NCs were finally formed after solvent extraction.

Fig. S2



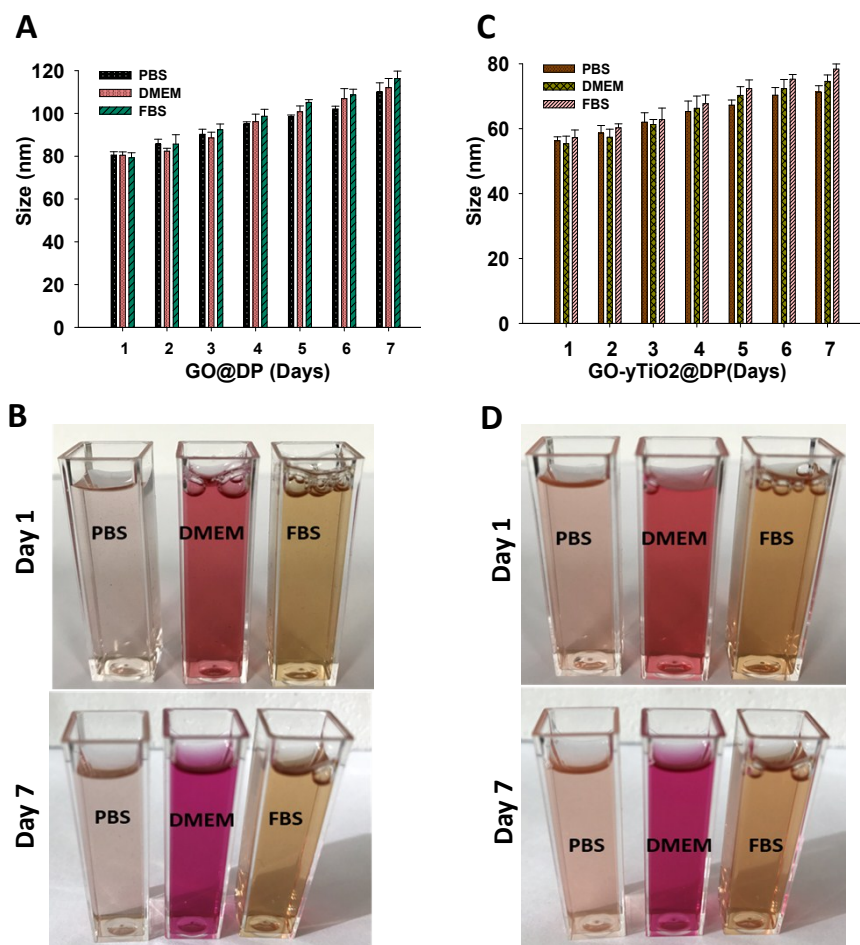
Powder and surface crystalline structures of base materials (yTiO₂ and GO). (A) XRD spectra of hydrogen flame-synthesized (TiO₂) and ultrasonically reacted (for 1 min) TiO₂ with H₂O₂ (yTiO₂). Inset: Digital images showing the sampled TiO₂ (left, white) and yTiO₂ (right, yellow) powders. (B) Raman spectra of TiO₂ and yTiO₂ powders. Insets: Optical microscope images of TiO₂ (upper, white) and yTiO₂ (lower, yellow) powders on glass discs. (C) XPS spectra of TiO₂ and yTiO₂ powders. Insets: Atomic ratios of Ti and O in TiO₂ and yTiO₂ powders. (D) C1s core spectrum GO incorporated with yTiO₂, D, and P.

Fig. S3



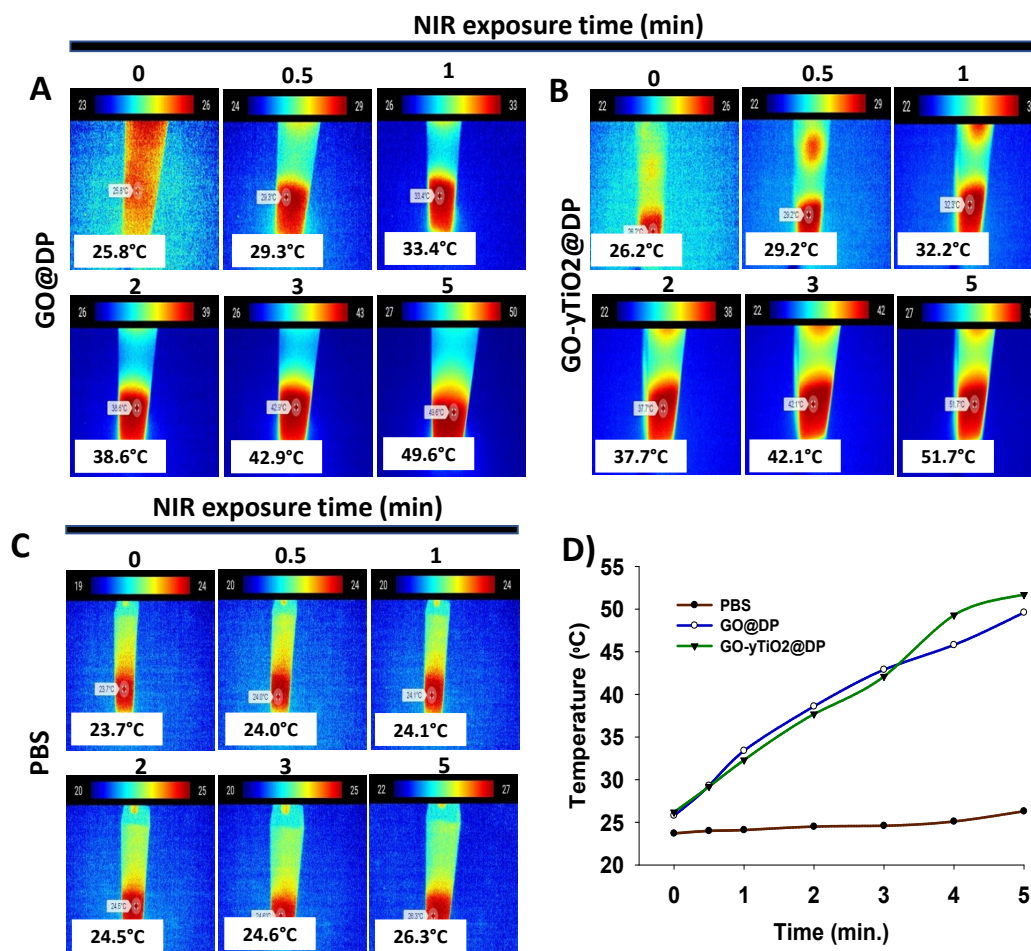
D loading performance of base materials (GO and GO-yTiO₂). (A) EE and LC of D on GO and GO-yTiO₂ in the absence of P. (B) UV-vis spectra of free D, GO@DP, and GO-yTiO₂@DP (50 $\mu\text{g}\cdot\text{D mL}^{-1}$). Inset: Digital image showing D, GO@DP, and GO-yTiO₂@DP dispersions.

Fig. S4



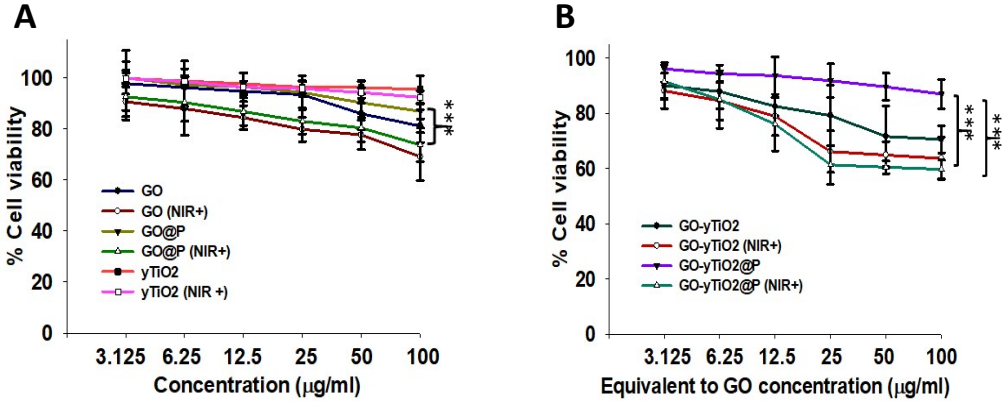
Dispersion stability measurements for GO@DP and GO-yTiO₂@DP dispersions. DLS results and digital images of (A, B) GO@DP and (C, D) GO-yTiO₂@DP dispersions (PBS, DMEM, and FBS) for 7-day measurements at room temperature.

Fig. S5



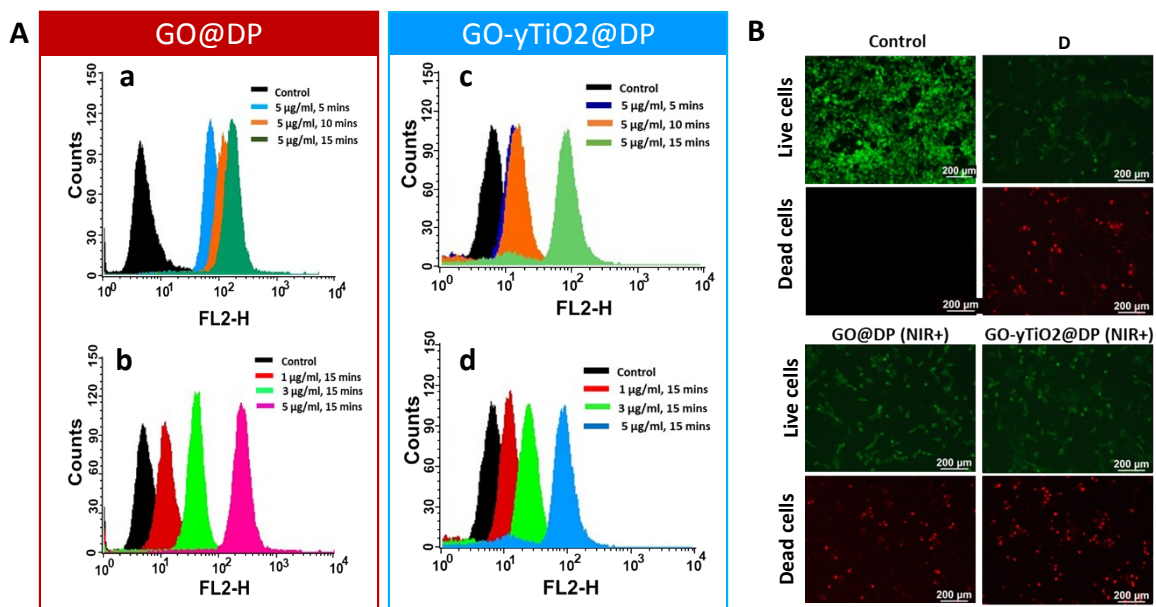
Photothermal activities of GO@DP and GO-yTiO₂@DP. NIR (808 nm, 2.0 W cm⁻² power density) was irradiated for 5 min on (A) GO@DP and (B) GO-yTiO₂@DP dispersions, including (C) saline (control), and the temperatures were recorded using thermal camera. (D) Summarized temperature elevation profiles of the dispersions as a function of NIR irradiation time.

Fig. S6



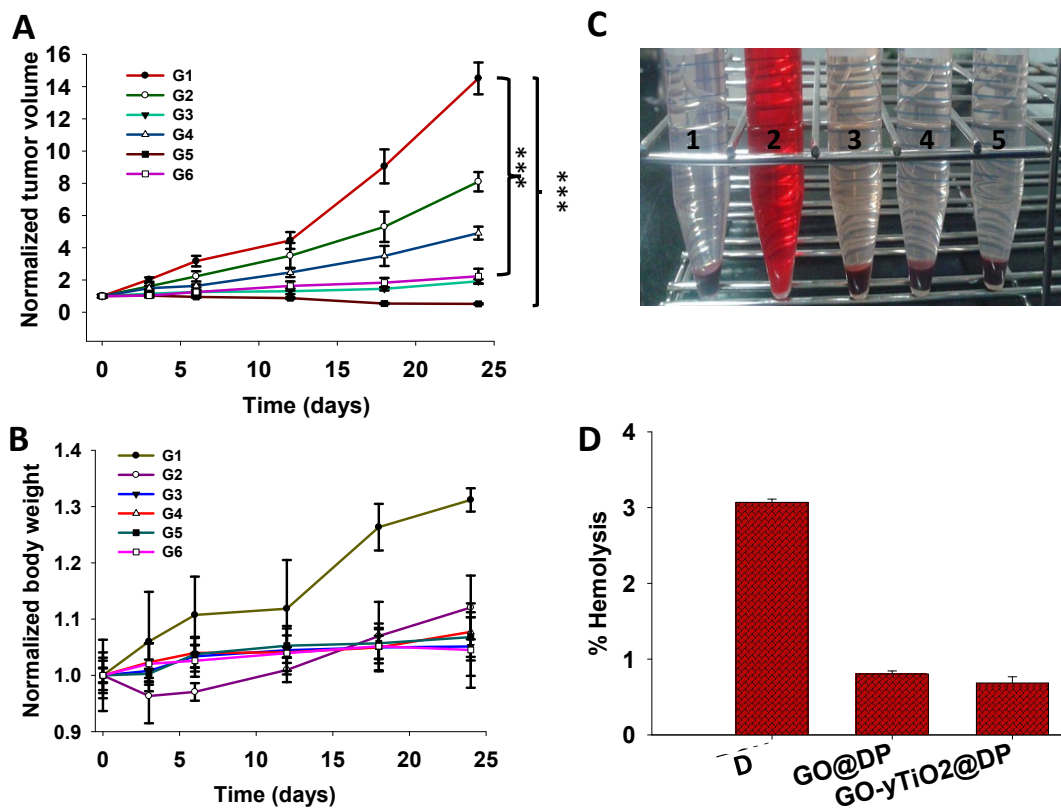
Cytotoxic response of SCC-7 cells after treatment with (A) GO, GO@P, and y-TiO₂ and (B) GO-yTiO₂ and GO-yTiO₂@P with or without NIR irradiation (***p* < 0.001).

Fig. S7



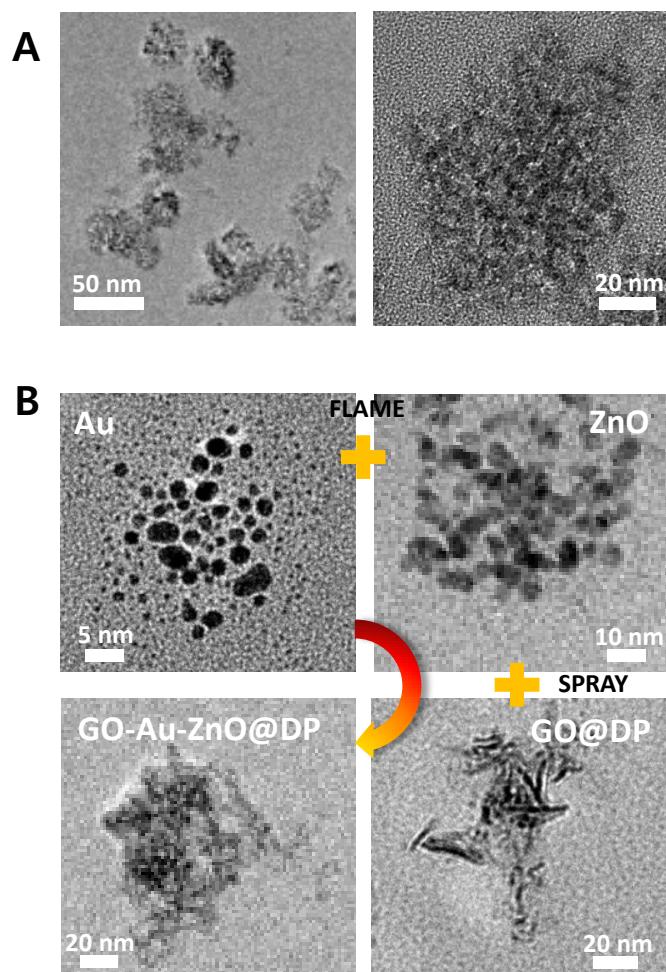
(A) FACS analyses for GO@DP and GO-yTiO₂@DP uptake into SCC-7 cells in a time-dependent (a, c: 5–15 min at 5 μg mL⁻¹) and a concentration-dependent (b, d; 1–5 μg mL⁻¹ at 15 min) manner. (B) Live and dead images of SCC-7 cells after treatment with free D, GO@DP, and GO-yTiO₂@DP with NIR irradiation (24 h incubation). Scale bars = 200 μm.

Fig. S8



Monitoring of (A) tumor volumes and (B) body weights of SCC-7 tumor bearing Balb/c nude mice following intravenous administration of the samples (G1: control; G2: D; G3: GO@DP + NIR; G4: GO@DP; G5: GO-yTiO₂@DP + NIR; G6: GO-yTiO₂@DP). Each sample was administrated three times at 3-day intervals ($***p < 0.001$). (C) Digital images (1: negative control; 2: positive control; 3: free D; 4: GO@DP; 5: GO-yTiO₂@DP) and (D) Percentage hemolysis on red blood cells (RBCs) treated with of free D, GO@DP, and GO-yTiO₂@DP incubated for 30 min at 37°C ($5 \mu\text{g} \cdot \text{D mL}^{-1}$). Absorbance of the samples was measured at 540 nm using a UV-vis spectrophotometer.

Fig. S9



TEM images of (A) GO-yTiO₂@DP from small-scale reactor (12 mg h⁻¹ capacity) and (B) GO-Au-ZnO@DP NCs from different flame pyrolysis using two precursors (gold[III]-chloride hydrate and zinc naphthenate) instead of titanium(IV) chloride. Au-ZnO NPs were incorporated with DP at a mechanical spray device containing GO and DP to form GO-Au-ZnO@DP.

TABLE S1

Summaries (geometric mean diameter [GMD], geometric standard deviation [GSD], and total number concentration [TNC]) of size distribution measured by SMPS for γTiO_2 , GO@DP, and GO- γTiO_2 @DP

	Geometric mean diameter (nm)	Geometric standard deviation	Total number concentration (cm^{-3})
γTiO_2	137.4508	1.7468	5.87E+06
GO@DP	156.1675	2.0527	1.44E+06
GO- γTiO_2 @DP	142.3817	1.9198	6.27E+06

TABLE S2

Histomorphometrical analyses of tumor mass, taken from tumor cells in xenograft athymic nude mice

Groups	Immunoreactive cell percentages (% mm^{-2} of tumor mass)			
	Cleaved caspase-3	Cleaved PARP	Ki-67	CD31 (PECAM-1)
Control (G1)	8.66±4.08	6.11±3.76	51.47±7.86	39.80±4.31
Treatment				
D (G2)	31.28±10.05 ^a	18.83±5.59 ^a	36.11±5.50 ^a	29.32±4.41 ^a
GO@DP NIR+ (G3)	58.71±5.79 ^{ab}	48.48±4.91 ^{ab}	19.72±2.61 ^{ab}	17.21±1.88 ^{ab}
GO@DP (G4)	46.41±5.70 ^{abd}	38.83±6.51 ^{abe}	29.52±2.95 ^{acd}	22.04±2.65 ^{abe}
GO- γTiO_2 @DP NIR+ (G5)	83.65±8.97 ^{abdf}	77.91±10.48 ^{abdf}	6.06±1.46 ^{abdf}	5.06±2.21 ^{abdf}
GO- γTiO_2 @DP (G6)	71.05±1.98 ^{abdfg}	64.12±4.41 ^{abdfh}	11.03±2.75 ^{abdfg}	11.28±2.35 ^{abdfg}

Values are expressed as mean ± SD of six tumor mass histological fields.

^a $p < 0.01$ as compared with G1 by MW test

^b $p < 0.01$ and ^c $p < 0.05$ as compared with G2 by MW test

^d $p < 0.01$ and ^e $p < 0.05$ as compared with G3 by MW test

^f $p < 0.01$ as compared with G4 by MW test

^g $p < 0.01$ and ^h $p < 0.05$ as compared with G5 by MW test

TABLE S3

Histopathological-histomorphometrical analyses of major organs, taken from tumor cells in xenograft athymic nude mice

Groups	Organs	Heart	Liver	Spleen	Lung	Kidney
		Abnormal finding				
Control (G1)		0/6 (0%)	0/6 (0%)	0/6 (0%)	0/6 (0%)	0/6 (0%)
Treatment						
D (G2)		0/6 (0%)	0/6 (0%)	0/6 (0%)	0/6 (0%)	0/6 (0%)
GO@DP NIR+ (G3)		0/6 (0%)	0/6 (0%)	0/6 (0%)	0/6 (0%)	0/6 (0%)
GO@DP (G4)		0/6 (0%)	0/6 (0%)	0/6 (0%)	0/6 (0%)	0/6 (0%)
GO- γTiO_2 @DP NIR+ (G5)		0/6 (0%)	0/6 (0%)	0/6 (0%)	0/6 (0%)	0/6 (0%)
GO- γTiO_2 @DP (G6)		0/6 (0%)	0/6 (0%)	0/6 (0%)	0/6 (0%)	0/6 (0%)

Values were numbers of abnormal fields/total observed fields (six histological fields in each group).